New Insights into the Mechanism of Oxidatively-Induced CO-Substitution Reaction in the Bimetallic $FvCo_2(CO)_4$ Gained by Digital Simulation Studies

Sameerah I. Al-Saeedi[1], Ali M. Alsalme[2] and Ayman Nafady[2,3]*

[1]Department of Chemistry, College of Science, Princess Nora bint Abdulrahman University, Riyadh, Saudi Arabia
[2]Department of Chemistry, College of Science, King Saud University, Riyadh, Saudi Arabia
[3]Department of Chemistry, Faculty of Science, Sohag University, Cairo, Egypt
[*]E-mail: anafady@ksu.edu.sa

In this study, digital simulations were performed for cyclic voltammograms (CV) obtained at different scan rates (0.2 to 1.0 V/s) for the oxidatively-promoted CO-substitution reaction by PPh_3 in the bimetallic $FvCo_2(CO)_4$,**1**, in CH_2Cl_2/0.05 M $[NBu_4][B(C_6F_5)_4]$ in order to establish the possible mechanism by which this reaction occurs. For the simulation input parameters, transfer coefficients (α) were kept at 0.5 and diffusion coefficients values of $D_o = 1.53 \times 10^{-5}$ and 1×10^{-5} cm^2 s^{-1} were used for **1** and the substitution product $FvCo_2(CO)_3PPh_3$, **2**, respectively. An associative mechanism that involves four heterogeneous electron-transfer reactions (k_s) for $\mathbf{1}^{0/+}$, $\mathbf{1}^{+/2+}$, $\mathbf{2}^{+/0}$, $\mathbf{2}^{+/2+}$, and two homogeneous chemical reactions (k_f) of $\mathbf{1}^+$ and $\mathbf{1}^{2+}$ with PPh_3 gave best fitting to the experimental CVs. Although the inclusion of the reaction between PPh_3 and $\mathbf{1}^{2+}$ only slightly improves the fitting, it suggests that the rates and equilibrium constants for CO-substitution processes in $\mathbf{1}^+$ and $\mathbf{1}^{2+}$ to be of the same order of magnitude. Importantly, the values of both K_{eq}^1 (k_f^1/k_b^1) and k_f^1 were shown to be quite large ($\geq 10^5$ M^{-1} and $\geq 5 \times 10^3$ M^{-1} s^{-1}, respectively). This finding clearly demonstrates that the substitution of CO by PPh_3 in the radical cation $\mathbf{1}^+$ is thermodynamically highly favored and kinetically rapid on the voltammetric time scale.

## 1. INTRODUCTION

Nucleophilic substitution reaction induced by electron-transfer (ET) has become an essential procedure for the synthesis and characterization of a wide range of inorganic and organometallic

compounds [1]. In this context, oxidatively-promoted PPh_3-for-CO ligand substitution in 18-electron half-sandwich metal carbonyl compounds is generally believed to occur via generation of the corresponding 17 electron cation, followed by rapid attack by the added nucleophile [2-6]. As seen, for instance, in the synthesis of $Cr(\eta^6\text{-arene})(CO)_2L$ (L = phosphite) complexes [7, 8], the facile CO-substitution by a more donating two-electron ligand (L) is facilitated by the diminished metal carbonyl-carbon bond strength that arises from reduced back-bonding in the 17-electron $[Cr(\eta^6\text{-arene})(CO)_3]^+$ cation [8]. Whether the substitution process is reductively or oxidatively promoted, catalytic or stoichiometric; the rate of the radical substitution reaction, k_{sub}, is crucial to success of the method [9]. Thus, several rate-determining studies based on analysis of cyclic voltammetry (CV) data have appeared in literature for half-sandwich systems [7-10]. Particularly relevant to the present paper are the studies of substitution rates of the congener $CpCo(CO)_2$ [11- 13] and various 'cymantrene'-type complexes having $Mn(CO)_2L$ moieties bonded to modified Cp $(\eta^5\text{-}C_5H_5)$ ligands [14].

In stark contrast to the intensive investigations on the substitution reactions of mono-nuclear metal carbonyl compounds, only few studies have been reported for the dinuclear congeners [15, 16]. In a previous paper [17], we have shown that the kinetic stability of the oxidized products of the bimetallic $FvCo_2(CO)_4$, **1**, in a gentle media comprising CH_2Cl_2 and weakly coordinating $[NBu_4][B(C_6F_5)_4]$ as supporting electrolyte enabled the substitution of a single carbonyl group (CO) by PPh_3 as detailed in reference [18]. As a result electrochemical and spectral characterization of the phosphino derivative $[Co_2Fv(CO)_3(PPh_3)]^{n+}$ in three different redox states (*n*) = 0, 1, 2 have been accomplished [18]. In the same paper, based on evidence gained by electrochemical as well as IR and ESR spectroscopy, we proposed a mechanism for the redox-promoted PPh_3-for-CO-substitution that takes into account the main reaction pathway (**1**$^+$ with PPh_3) along with other plausible pathways including **1**$^{2+}$ with PPh_3 and **2**$^+$ or **2**$^{2+}$ with PPh_3 as illustrated in Scheme 1 [18].

.
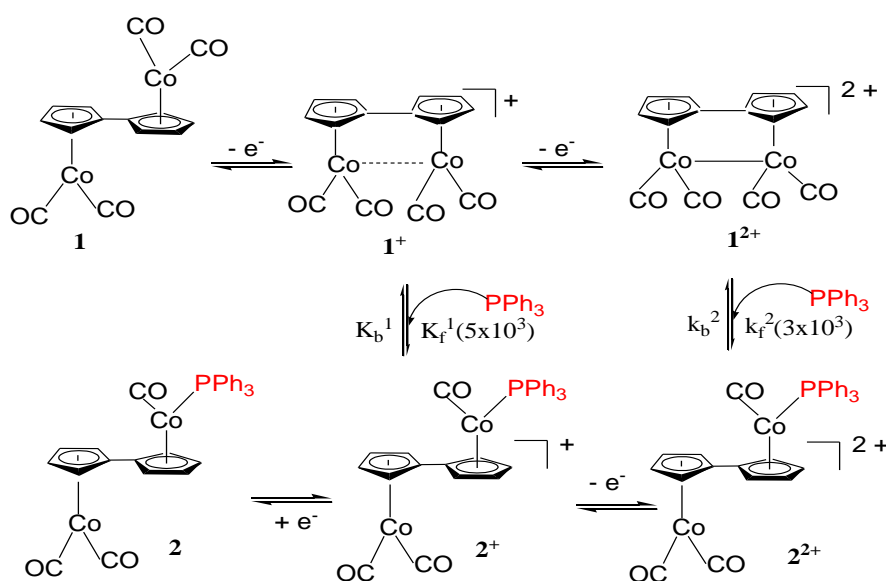
Scheme 1. Showing the heterogeneous electron-transfer and homogeneous CO-substitution reaction by PPh_3 in $FvCo_2(CO)_4$ complex

Compared with mononuclear analogues [9-13], the complexity of the substitution reaction in dinuclear complexes containing two equivalent redox centers and more than one CO ligand arises from the fact that there is more than one possible pathway for the second phosphine (PPh_3) to attack the substrate. This means, it is possible for the second PPh_3 to attack either the first substituted center (leading to a di-substitution product on one side of the complex) or to replace one of the CO groups at the second cobalt center of the $FvCo_2(CO)_4$, **1**, thereby generating a product with two equivalent mono-substituted centers. Thus, in order to theoretically discern the likely mechanism(s) involved in this oxidatively-induced PPh_3-for-CO substitution reaction in **1** and to determine the thermodynamic and kinetic parameters associated with the underlying homogeneous (k_f) and heterogeneous (k_s) reactions, detailed digital simulation studies on the generated cyclic voltammograms have been undertaken in this paper

2. EXPERIMENTAL

The experimental work was conducted at Prof. W. E. Geiger's laboratory at the University of Vermont, USA.

All experiments were performed under nitrogen using either standard Schlenk techniques or a Vacuum Atmospheres drybox. Reagent-grade dichloromethane (CH_2Cl_2) is dried over CaH_2 and then vacuum distilled. $FvCo_2(CO)_4$, **1**, had been prepared based on a literature procedure [17]. $[NBu_4][B(C_6F_5)_4]$ was prepared by metathesis of $[NBu_4]Br$ with $K[B(C_6F_5)_4]$ (Boulder Scientific, Boulder, Co) and purified as detailed elsewhere [19]. Electrochemical measurements were undertaken inside a drybox using a standard three-electrode cell configuration and a PARC 273A potentiostat interfaced to a personal computer. The glassy carbon working electrodes (1.5 mm diameter, Cypress, or 1 mm diameter, from Bioanalytical Systems) are routinely polished with Buehler diamond paste, followed by washings with nanopure water, and dried under vacuum. The working electrode for bulk electrolysis was a Pt-basket.

All potentials in this paper are referenced versus ferrocene/ferrocenium($Fc^{0/+}$) couple. Mechanistic aspects associated with the redox processes were performed using cyclic voltammetry (CV) and linear sweep voltammetric (LSV) data. Diagnostic criteria such as shapes and scan rate responses of the CV curves were accomplished via protocols described in reference [20]. The data was simulated using the fitting procedure of Digsim 3. IR spectra were recorded with an ATI-Mattson Infinity Series FTIR interfaced to a computer, using Winfirst software at a resolution of 4 cm^{-1}.

3. RESULTS AND DISCUSSION

3.1 Identifying the Nature of CO-Substitution and Possible Pathways

Before going into details about the digital simulation studies of the cyclic voltammetric data generated during the course of redox-promoted CO-substitution reaction by PPh_3 for the bimetallic $FvCo_2(CO)_4$, **1**, in media composing of $CH_2Cl_2/[NBu_4][B(C_6F_5)_4]$, it is important, from practical point

of view, to address two major points. Firstly, to deduce whether this reaction is catalytic or stoichiometric in nature and secondly to figure out if the CO-substitution by PPh$_3$ follows an associative and dissociative pathway to generate the final PPh$_3$-substitution product. In addressing the first point, however, it is important to emphasize that oxidatively induced CO-substitution, in general, would not be expected to be catalytic because the product will have an E$_{1/2}$ negative of the reactant's E$_{1/2}$ [21]. The first evidence was directly obtained by examining the cyclic voltammetric behavior of **1** in the absence and the presence of added nucleophile, PPh$_3$, at different applied switching potentials. Figure 1(a) shows the effect of switching potentials on the CVs of **1** in presence of 1 equiv of PPh$_3$ at scan rate of 100 mV/s. This figure represents a typical illustration of cyclic voltammetric behavior that is not electrocatalytic in nature since applying of positive potentials that are less than E$_{1/2}$ of **1/1**$^+$ couple and scanning back to more negative potentials does not lead to any appreciable detection of the substitution product **2**$^+$/**2** (E$_{1/2}$ = -0.35 V). Formation of this product was only observed when the applied potential is equal to or exceeds the E$_{1/2}$ of the first oxidation wave of **1**. This means, complete conversion of **1** to **1**$^+$ is very necessary for this reaction to occur. Also closer inspection of the CV data of **1** before and after addition of PPh$_3$ Fig. 1(b), reveals that the anodic current of the first oxidation wave of **1** before and after addition of 1 equiv PPh$_3$ is nearly constant. Virtually, this observation does not support a redox catalytic process. Instead, it suggests a kinetic phenomenon in which **1**$^+$ is itself consumed in a bimolecular reaction with the added PPh$_3$ to afford the mono-substituted product, **2**$^+$, in the region adjacent to the electrode. This is clearly evidenced by the appearance of the waves corresponding to either its oxidation to a dication **2**$^{2+}$ or reduction to the neutral compound **2** (depending on the direction of scanning the potential).
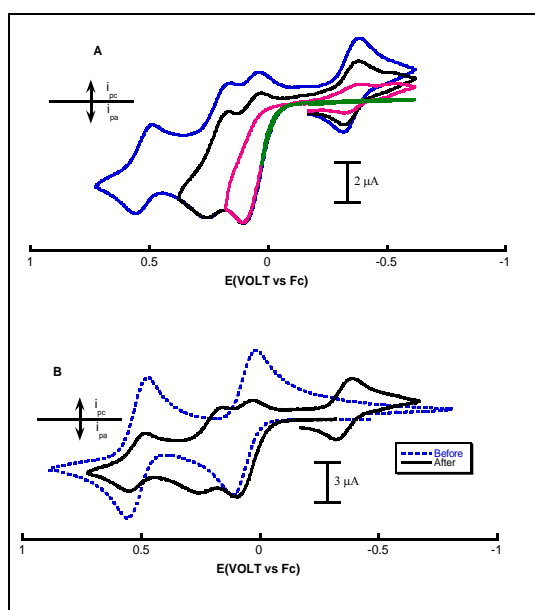
Figure 1. (a) Cyclic voltammograms obtained at different switching potentials for 1 mM **1** in CH$_2$Cl$_2$/0.05 M [NBu$_4$][B(C$_6$F$_5$)$_4$] at scan rate of 100 mV/s, 1 mm GC disk electrode. (b) Cyclic voltammograms of 1.5 mM **1** in CH$_2$Cl$_2$/0.05 M [NBu$_4$][B(C$_6$F$_5$)$_4$] at scan rate of 100 mV/s, 1 mm GC disk electrode before and after the addition of 1 equiv PPh$_3$.

The second evidence for the absence of catalysis in this electrochemically-induced CO-substitution reaction stems from the fact that electrocatalysis of ligand substitution is best illustrated by either examining the effect of an extremely small anodic current upon solutions of reactants containing added nucleophile or by performing bulk electrolysis and observing the coulomb count [22]. Thus, for truly catalytic processes complete conversion of reactants into products require substantially less than 1 Faraday of charge per mole of reactants during bulk electrolysis of the substrate in the presence of added nucleophile [23]. Applying this approach to the bulk electrolysis of **1** in presence of PPh$_3$ reveals that the electrolysis was completed upon consumption of approximately 2 Faraday of charge per 1 mole of the compound. As illustrated in reference [17, 18] the coulomb count is accounted for by the successive one-electron oxidation of **1** followed by one-electron oxidation of the generated product **2**$^+$ to **2**$^{2+}$. Thus, in view of the conclusions drawn from the transient and bulk techniques, it is clearly established that the process of CO- substitution by PPh$_3$ in the bimetallic FvCo$_2$(CO)$_4$, **1**, system is a stoichiometric rather than catalytic in nature.
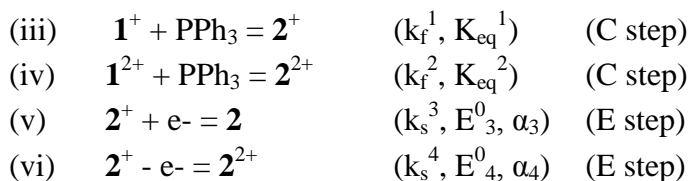
Turning to the second point, which deals with the mechanism involved in this electrochemically-induced CO-substitution reaction, in principle, there are two possible mechanisms with either *associative* or *dissociative* pathways. In the case of FvCo$_2$(CO)$_4$, **1**, the associative pathway would involve removal of an electron from the neutral compound to generate the monocation, **1**$^+$, which is then rapidly attacked by the nucleophile, PPh$_3$, to afford the monosubstituted monocation, **2**$^+$, with the loss of one CO ligand (see Scheme 1). This **2**$^+$ can then be oxidized to a dication, **2**$^{2+}$ upon losing a second electron or reduced to neutral **2**, upon - uptake of an electron. However, if substitution takes place through a dissociative pathway, this would involve loss of CO from the monocation **1**$^+$ prior to reaction with the added nucleophile. The fact that **1**$^+$ is persistent in solution when generated in the absence of PPh$_3$ [17] excludes the possibility of losing CO from **1**$^+$ and therefore, the substitution reaction of CO by PPh$_3$ upon electrochemical oxidation of **1** appears to be *associative* in nature. In order to confirm this conclusion and to estimate the thermodynamic and kinetic parameters of these homogeneous and heterogeneous reactions, we now turn to digital simulation of the experimental cyclic voltammetric data obtained during anodic oxidation of the bimetallic FvCo$_2$(CO)$_4$, **1**, in the presence of 1 equiv PPh$_3$ at different scan rates and concentrations.

3.2 Digital Simulations of Cyclic Voltammetry

3.2.1. Digital Simulation of a Mechanism Involving either One or Two Chemical Steps

The data chosen for simulations is a series of background-subtracted cyclic voltammograms of 1.1 mM **1** in the presence of 1 equiv PPh$_3$ at different scan rates (0.2 to 1 V/s). Ohmic loss in the experimental CVs was partially compensated by applying positive feedback. The data was simulated using the fitting procedure of Digsim 3 (see experimental). The simulation was started out by making the assumption that CO-substitution is possible for both the monocation **1**$^+$ and the dication **1**$^{2+}$, and that the mechanism by which this substitution reaction occurs is *associative* as illustrated in Scheme 2.

  (i)   **1** - e$^-$ = **1**$^+$ (k$_s^1$, E$^0_1$, α$_1$)   (E step)
  (ii)   **1**$^+$ - e$^-$ = **1**$^{2+}$ (k$_s^2$, E$^0_2$, α$_2$)   (E step)

(iii)	$\mathbf{1}^+ + PPh_3 = \mathbf{2}^+$		(k_f^1, K_{eq}^1)	(C step)	
(iv)	$\mathbf{1}^{2+} + PPh_3 = \mathbf{2}^{2+}$		(k_f^2, K_{eq}^2)	(C step)	
(v)	$\mathbf{2}^+ + e- = \mathbf{2}$		(k_s^3, E_3^0, α_3)	(E step)	
(vi)	$\mathbf{2}^+ - e- = \mathbf{2}^{2+}$		(k_s^4, E_4^0, α_4)	(E step)	

Scheme 2. Showing the mechanism used for digital simulation of the CV data.

As seen in our previous work on this system [17, 18], the generated cyclic voltammograms exhibit four reversible waves; two for oxidation of **1** to the corresponding $\mathbf{1}^+$ and $\mathbf{1}^{2+}$ (eqs i, ii) cation [17] and two for the substitution product, $\mathbf{2}^+$ (eqs v, vi) [18]. This implies that the proposed mechanism must include four electron-transfer reactions (k_s^{1-4}) as well as two homogeneous chemical reactions ($k_f^{1,2}$ and $K_{eq}^{1,2}$) between the generated cations $\mathbf{1}^+$ and $\mathbf{1}^{2+}$ with added nucleophile, PPh_3 (eqs iii, vi). Accurate simulations of this complex mechanism require knowledge of $E_{1/2}$, the formal potential of the redox couples of the parent compound and the substitution product i.e., $\mathbf{1/1}^+$, $\mathbf{1}^+/\mathbf{1}^{2+}$, $\mathbf{2}^+/\mathbf{2}^{2+}$ and $\mathbf{2}^+/\mathbf{2}$, as well as their intrinsic heterogeneous electron-transfer rate constants (k_s); the homogeneous rate constants (k_f^1, k_f^2) for ligand exchange; the diffusion coefficients D of both **1** and **2**; the transfer coefficient α; and the initial concentration of **1** and added PPh_3.

The formal potentials E^0 are well approximated by the CV peak parameters and expressed as $E^0 = (E_{pa} + E_{pc})/2$ for the reactant **1** and the substitution product **2.** The heterogeneous electron transfer rates, k_s, for **1** were determined previously to be 0.015 and 0.02 cm/s for the first and second redox couple, respectively [17]. Since the diffusion coefficients are not highly structural-dependent, species ($\mathbf{1}^+$, $\mathbf{1}^{2+}$) were given the same value of D as **1** = 1.53 x 10^{-5} cm^2/s. The diffusion coefficients of the species **2**, $\mathbf{2}^+$, $\mathbf{2}^{2+}$ were similarly estimated to be 1 x 10^{-5} cm^2/s based on the fact that a PPh_3 ligand is expected to make the D value lower. The effective electrode area, A, was evaluated to be 0.078 cm^2. The transfer coefficients, α, are 0.5 for all species, as qualitatively indicated by the symmetry of the reversible waves [21].

The fitting sequence typically involves fitting each parameter individually and then fitting the parameters in sets. We started out by first fitting the electrochemical parameters E^0, k_s, and α for each redox couple of **2** by choosing an intuitive estimate of $k_f^1 = 5$ x 10^3 M^{-1} s^{-1}, $K_{eq} = 1$ x 10^5 M^{-1} for 1.1 x 10^{-3} M **1** and 1.1 x 10^{-3} M PPh_3 (1 equiv), scan rate = 0.5 V/s. Each electrochemical parameter was then systematically varied to determine its effect on the cyclic voltammogram. The optimization process was repeated until the simulated values were constant within the experimental accuracy (typically 2 or 3 significant figures). Table 1 lists the electrochemical parameters of the substitution product that gives best fitting. These simulations began with the assumption that the values of the K_{eq} are quite large, favoring the forward (CO-substitution) reactions in Scheme 2, and a value of 1 x 10^{-5} M^{-1} was used for both K_{eq}^1 and K_{eq}^2. Under this assumption, k_f^1 value that gives the best fit was 5 x 10^{-3} M^{-1}s^{-1}. Similarly, the kinetic parameters of the second homogeneous substitution reaction (k_f^2, eq iv) were measured.

Figure 2(a) shows the effect of systematically increasing the values of k_f^2 from 10 M^{-1} s^{-1} to 1 x 10^4 M^{-1} s^{-1}. The value of k_f^2 that gives best fitting to the experimental CVs is found to be 3 x 10^3 M^{-1} s$^-$

[1]. This value quantitatively represents the upper limit of k_f^2 since lower values of k_f^2 (10 to 2 x 10^{-3}) always give larger cathodic currents of the reverse scan than the experimental CVs; also increasing the value of k_f^2 to one equals to k_f^1, 5 x 10^3, or larger 1 x 10^{-4} M^{-1} s^{-1} results in less cathodic current for the two reduction waves of $2^{2+}/2^+$ and $2^+/2$ couples, thereby leading to a very poor fitting between the simulated and experimental CVs as illustrated in Figure 2(a). Consistent with our previous work [17], this finding indicates that the rate of CO-substitution by PPh_3 at the dication, 2^{2+} might be slower than that of the monocation, 2^+.

The same systematic study was also applied to study the effect of K_{eq}^2 on the simulated CVs. Figure 2(b) shows that values smaller than 1 x 10^5 always result in larger cathodic currents for the reverse waves while, larger values of K_{eq}^2 give the same fitting, meaning that this value for the equilibrium constant represents the lower limit that gives best fitting. Tables 1(a) and 1(b) list the parameters of the heterogeneous and homogeneous reactions that give best fitting to the experimental cyclic voltammograms at different scan rates as shown in Figure 3. These values are in a good agreement with those reported in ref. 17.
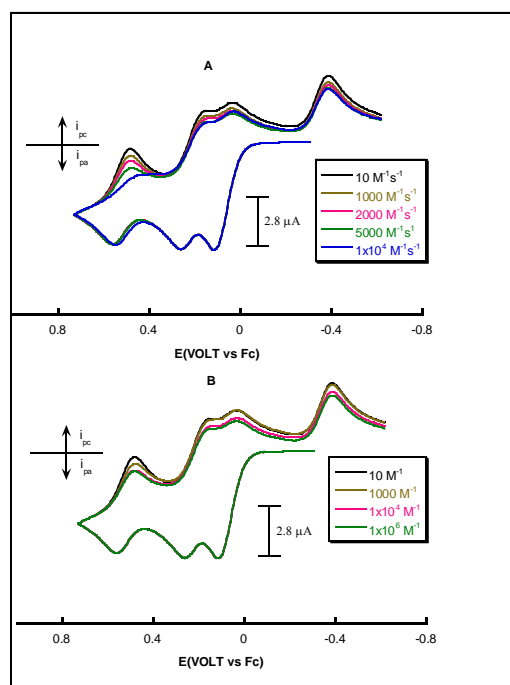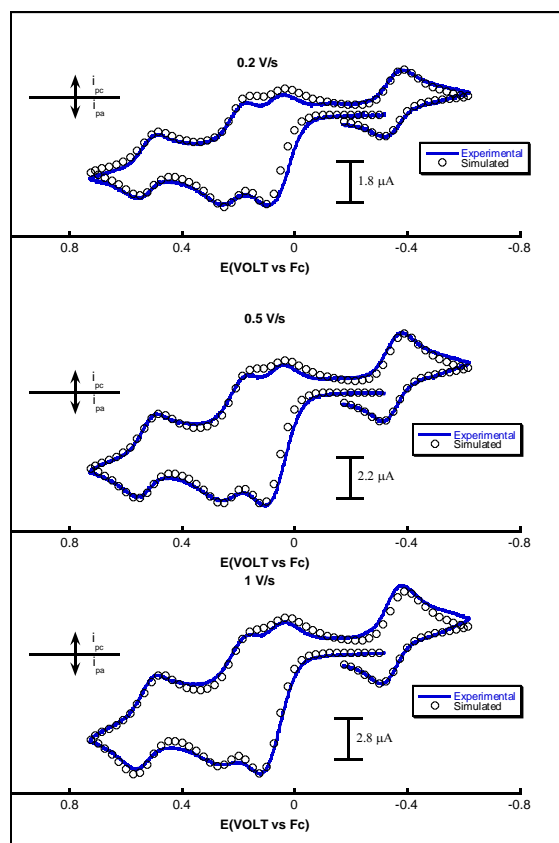

Figure 2. Simulated cyclic voltammograms of 1.1 mM **1** and 1 equiv PPh_3 at scan rates of 500 mV/s, (a) Effect of k_f^2 values on the simulated CVs (b) Effect of K_{eq}^2 values on the simulated CVs.

Table 1a. Digital Simulation Parameters for the Heterogeneous Electron Transfer Reactions of $FvCo_2(CO)_4$ and the substitution product $[FvCo_2(CO)_3PPh_3]$

comp	E^0_1 (V)	k_s^1 (cm/s)	α_1	E^0_2 (V)	k_s^2 (cm/s)	α_2
1	0.065	1.5×10^{-2}	0.5	0.510	2.0×10^{-2}	0.5
2	0.20	1.0×10^{-2}	0.5	-0.355	2.5×10^{-2}	0.5

Table 1b. Digital Simulation Parameters for the Homogeneous Chemical Reactions

k_f^1 ($M^{-1}s^{-1}$)	k_b^1 ($M^{-1}s^{-1}$)	K_{eq}^1 (M^{-1})	k_f^2 ($M^{-1}s^{-1}$)	K_b^2 ($M^{-1}s^{-1}$)	K_{eq}^2 (M^{-1})
5×10^3	5×10^{-2}	1×10^5	3×10^3	2×10^{-2}	1×10^5

Figure 3. Experimental and simulated cyclic voltammograms of 1.1 mM **1** in CH_2Cl_2/0.05 M [NBu$_4$][B(C$_6$F$_5$)$_4$] and 1 equiv PPh$_3$ at different scan rates on a 1 mm GC disk electrode. The two possible chemical steps are included in the simulation

Importantly, few points regarding the data in Table 1(b) should be considered. First, large values for the equilibrium constants K_{eq} of the two homogeneous reactions were employed, in order to obtain very good fitting between the experimental CVs and theory. This testifies that the proposed substitution products are thermodynamically favored and the possibilities of back reactions are extremely low. Second, the general shape of the simulated CVs is highly dependent on the k_f and K_{eq} values of the first CO-substitution reaction. Increasing k_f^1 values by the range of 1×10^2 to 1×10^4 $M^{-1}s^{-1}$ result in a dramatic change in the general shape of the simulated CVs as illustrated in Figure 4. As concluded in our previous work on the preliminary simulation of this mechanism, the value of k_f^1 that gives best fitting to experimental CVs at all scan rates used is found to be 5 $\times 10^3$ $M^{-1}s^{-1}$ [17]. Increasing this value to 8×10^3 M^{-1} s^{-1} or higher increases the anodic current of the substitution product (**2$^+$**/**2^{2+}**) couple and minimizes the anodic current of the second oxidation wave of the parent compound ($E_{1/2}$ = 0.51 V), leading to large disagreement between the experimental and simulated CVs. The same

effect was also observed upon gradually decreasing K_{eq}^1 from (1×10^5 M^{-1}) by an order of magnitudes as shown in Figure 5, where values smaller than 1×10^5 M^{-1} are shown to be inappropriate.
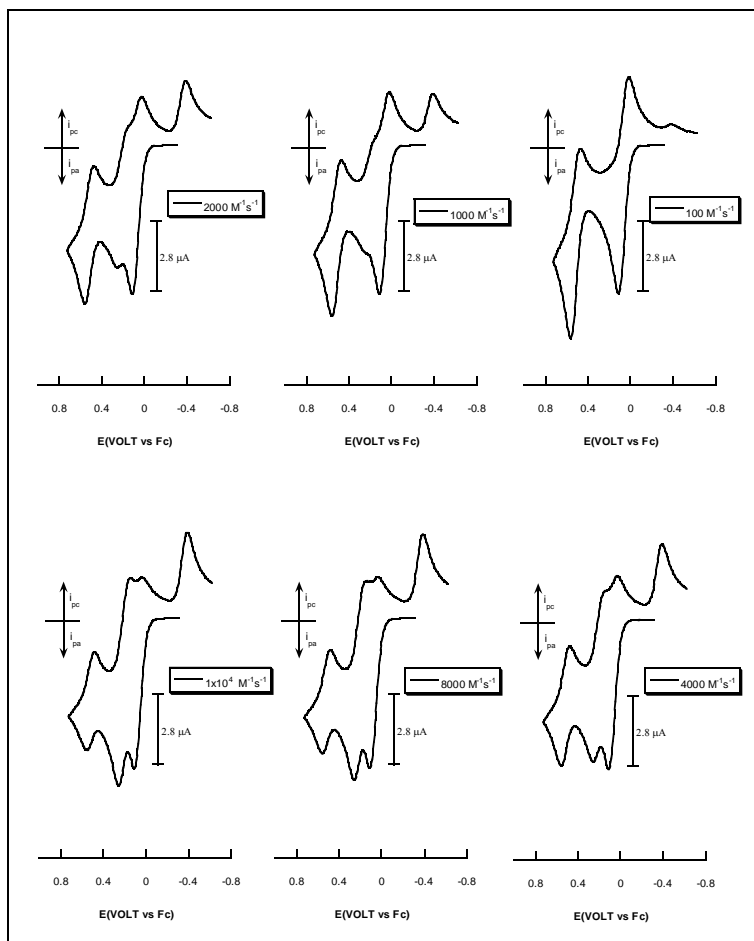
Figure 4. Simulated cyclic voltammograms of 1.1 mM **1** and 1 equiv PPh$_3$ at scan rate of 500 mV/s and different k_f^1 values.

Although kinetic parameters (k_f^2 and K_{eq}^2) of the second homogeneous chemical reaction (reaction of **1**$^{2+}$ with PPh$_3$) do not have the same influence on the general shape of the simulated CVs as shown in Figure 2, its inclusion in the mechanism is very important and useful in two ways. First, it is necessary to account for the large cathodic current on the reverse scan of the simulated CVs when this reaction is not included in the simulated mechanism as illustrated in Figure 6. Second, it gives a reasonable estimate for the homogeneous rate constant (k_f^2) of the dication, **1**$^{2+}$ (3×10^3 M^{-1} s^{-1}), which is useful in considering the comparative CO-substitution rates at the mono- and dication of **1** (**1**$^+$ and **1**$^{2+}$). Although both substitution reactions are fast, the smaller value of k_f^2 indicates that CO-substitution in **1**$^+$ species is more facile than that observed for **1**$^{2+}$. This can be readily explained in terms of the structural differences between **1**$^+$ and **1**$^{2+}$. In case of **1**$^{2+}$, the reaction involves uptake of the 2 e$^-$ donor PPh$_3$ and cleavage of the metal-metal bond, a process expected to slow the reaction [17].

Whereas, in the case of the monocation, 1^+, only partial formation of the Co-Co bond is anticipated and therefore its tendency to accommodate the upcoming PPh$_3$ would be much faster as illustrated in Scheme 1.
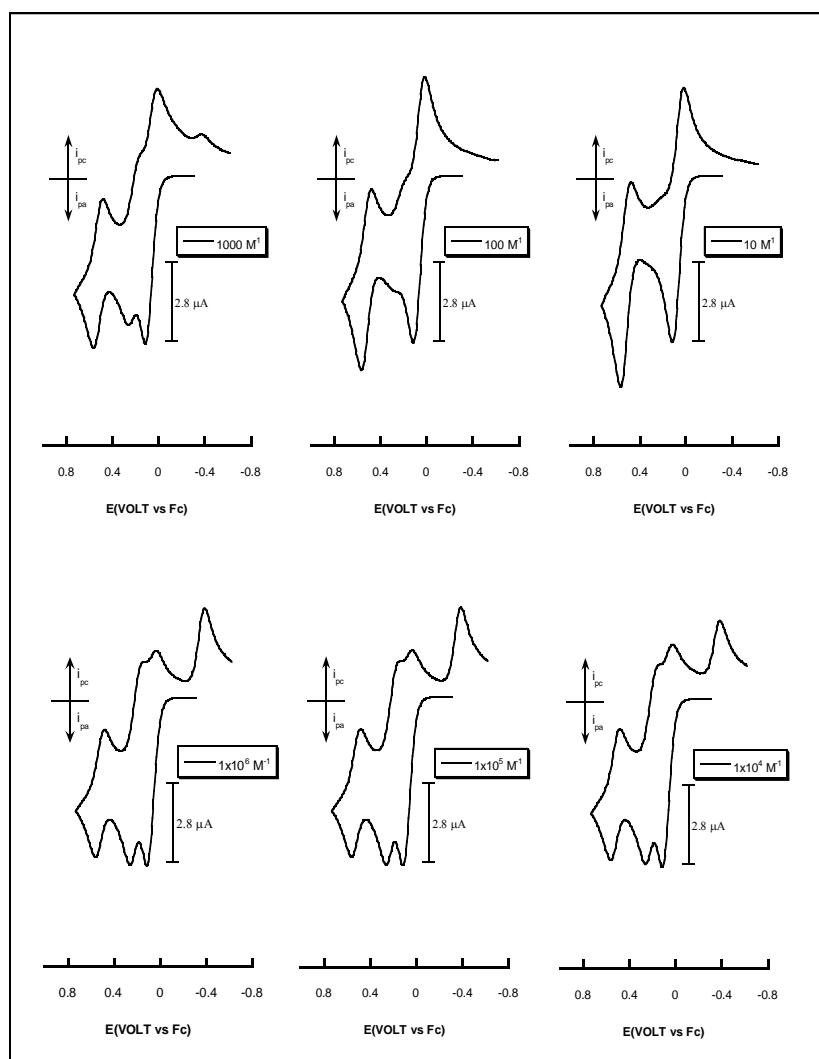
Figure 5. Simulated cyclic voltammograms of 1.1 mM **1** and 1 equiv PPh$_3$ at scan rate of 500 mV/s and different values of K$_{eq}$[1].

Taken together, the combined simulation results clearly established that the oxidatively-induced CO-substitution reaction by PPh$_3$ for the bimetallic FvCo$_2$(CO)$_4$, **1**, complex is best described by an associative mechanism that involves competitive substitutions of the carbonyl groups by the added PPh$_3$ at the monocation, 1^+, and dication, 1^{2+} to afford the monosubstituted product, [FvCo$_2$(CO)$_3$PPh$_3$]$^+$, 2^+ as the major final product. This finding is consistent with preliminary simulation studies performed on the system [17].
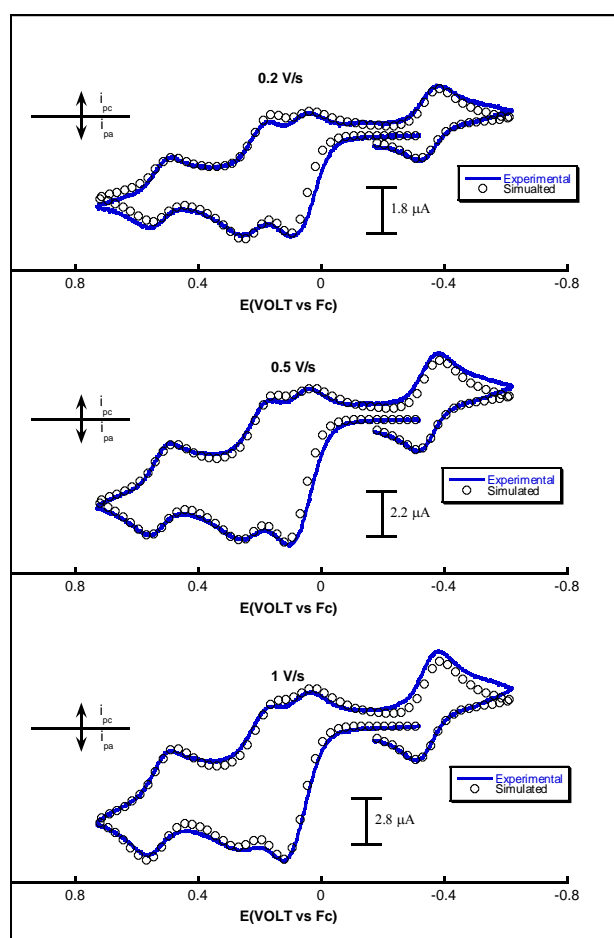
Figure 6. Experimental and simulated cyclic voltammograms of 1.1 mM **1** in CH_2Cl_2/0.05 M [NBu₄][B(C₆F₅)₄] and 1 equiv PPh₃ at different scan rates on a 1 mm GC disk electrode simulated without including the second chemical reaction.

3.2.2. Digital Simulation of a Mechanism Involving Three Chemical Steps

According to the assumption that the dicarbonyl part of each cationic side in **1** maybe substitution-prone to form PPh₃-substitution products, then it might be possible for the monosubstituted dication, 2^{2+}, to undergo further substitution reaction to afford the disubstituted dication, I^{2+}, as illustrated in Scheme 3.
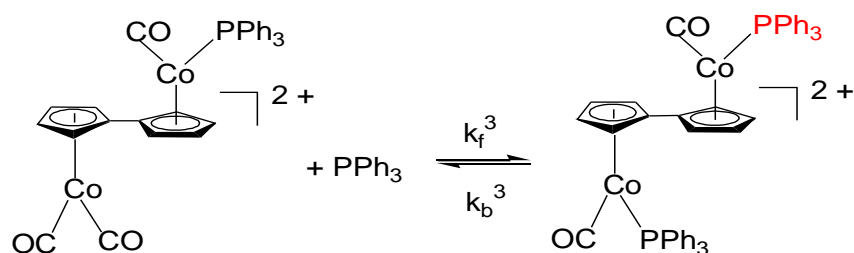
Scheme 3. Showing the possible reaction of the mono-substituted dication, 2^{2+} with PPh₃

Including this homogeneous chemical reaction in the proposed associative mechanism described in Scheme 2 means increasing the number of variables by two since values for k_f^3 and K_{eq}^3 must be included in the parameters set. Simulation of this mechanism, which now includes eighteen variables, adds a great deal of complexity to the proposed mechanism. However, after successful optimization of the parameters we obtained a satisfactory set of values that gives good fitting to the experimental CVs.

It is noteworthy that the optimized kinetic parameters for both k_f^3 and K_{eq}^3 of the homogeneous reaction between the dication of the substitution product 2^{2+} and PPh$_3$ are significantly different within the same parameter set. In other words, we obtained two sets of parameters for k_f^3 and K_{eq}^3 that give reasonable fitting to the experimental CVs as $K_{eq}^3 = 1\times10^5$ M^{-1} and $k_f^3 = 1.5\times10^2$ M^{-1}s^{-1} or $K_{eq}^3 = 4\times10^2$ M^{-1} and $k_f^2 = 3\times10^3$ M^{-1}s^{-1}. Indeed, the discrepancy encountered with the inclusion of this reaction on the proposed mechanism and its minimal role on the overall shape of the simulated cyclic voltammograms leads us to conclude that although this reaction might take place, its existence under these experimental conditions is not necessary to account for the observed CV behavior.

Although preliminary simulation data on a proposed simple mechanism, which includes only the reaction of the electrochemically generated monocation, 1^+, with the added PPh$_3$ to afford the mono-substituted phosphine product 2^+ had been appeared in literature [17], the complexity and the possible reaction of PPh$_3$ with more than one species in solution including 1^{2+}, 2^+ and 2^{2+} heightened the needs for more detailed simulation studies on this system as illustrated in this work. However, the combined simulation data, obtained by including various reaction pathways clearly demonstrate that care must be taken when attempting to optimize a large number of homogeneous and heterogeneous parameters in such a complex mechanism to satisfy the simulation conditions. Since the experimental requirements to measure these kinetic parameters are very complex, this example shows the benefits of using digital simulation of the cyclic voltammograms in deducing the possible mechanism for the electrochemically induced CO-substitution reaction and provides reasonable estimate for the thermodynamic and kinetics parameters associated with this complex mechanism.

4. CONCLUSION

In this study, extensive digital Simulations were conducted on background-subtracted cyclic voltammograms generated via an oxidatively-promoted CO-substitution reaction of the bimetallic FvCo$_2$(CO)$_4$, **1**, in CH$_2$Cl$_2$/0.05 M [NBu$_4$][B(C$_6$F$_5$)$_4$] in the presence of 1 equiv PPh$_3$ at different scan rates (0.2 to 1.0 V/s). The proposed mechanism that gave best fitting to the experimental CVs data for this substitution reaction is an associative mechanism having four electron-transfer and to chemical steps. The four heterogeneous electron-transfer reactions (k_s^{1-4}) are for the redox couples of the starting material (**1/1$^+$**, **1$^+$/1^{2+}**) and the generated substitution product (**2$^+$/2^{2+}** and **2$^+$/2**), whereas two homogeneous chemical reactions ($k_f^{1,2}$ and $K_{eq}^{1,2}$) are the reactions between the generated cations **1$^+$** and **1^{2+}** with PPh$_3$. Although inclusion of the latter reaction (**1^{2+}** with PPh$_3$) in the simulation only slightly improves the fitting between experimental CVs and theory, it allows for qualitative comparison between the substitution rates and equilibrium constants for reactions involving both **1$^+$**

and 1^{2+}. Importantly, the values of both K_{eq}^1 and k_f^1 were shown to be large ($\geq 10^5$ M^{-1} and $\geq 5 \times 10^3$ M^{-1} s^{-1}, respectively), thereby confirming that the substitution of CO by PPh$_3$ in the radical cation 1^+ is thermodynamically highly favored and kinetically rapid on the voltammetric time scale. The findings of this study heightened the benefits of performing digital simulations on cyclic voltammetric data when it becomes hard to determine experimentally the associated kinetic and thermodynamic parameters of the underlying process.

References

1. R.A. Rossi, A.B. Pierini, A.B. Penenory, *Chem. Rev.*, 103 (2003) 71–168
2. M.E. Rerek, F. Basolo, *J. Am. Chem. Soc.*, 106 (1984) 5908–5912
3. M.C. Baird, *J. Organomet. Chem.* 751 (2014) 50
4. J.W. Hershberger, J.K. Kochi, *J. Chem. Soc. Chem. Commun.* (1982) 212.
5. J.W. Hershberger, R.J. Klingler, J.K. Kochi, *J. Am. Chem. Soc.* 104 (1982) 3034.
6. T.R. Herrinton, T.L. Brown, *J. Am. Chem. Soc.* 107 (1985) 5700.
7. L.K. Yeung, J.E. Kim, Y.K. Chung, P.H. Rieger, D.A. Sweigart, *Organometallics* 15 (1996) 3891.
8. N.C. Ohrenberg, L.M. Paradee, R.J. Dewitte III, D. Chong, W.E.Geiger, *Organometallics* 29 (2010) 3179.
9. K. Wu, D.R. Laws, A. Nafady, W.E. Geiger, *J. Inorg. Organomet. Polym.* 24 (2014) 137.
10. N. Camire, A. Nafady, W. E. Geiger, *J. Am. Chem. Soc.* 124 (2002) 72*60.*
11. A. Nafady, P. J. Costa, M. J. Calhorda, W. E. Geiger, *J. Am. Chem. Soc.*128 (2006) 16587.
12. A. Nafady, W. E. Geiger, *Organometallics* 29 (2010) 4276**.**
13. A. Nafady, R. A. Ammar, H. M. El Sagher, U. A. Rana, K. A. AL-Farhan *Int. J. Electrochem. Sci.* 8 (2013) 1700.
14. W.E. Geiger, *Coord. Chem. Rev.* 257 (2013) 1459.
15. R.T. Baker, J.C. Calabrese, P.J. Krusic, M.J. Therien, W.C. Trogler, *J. Am. Chem. Soc.*, 110 (1988) 8392.
16. M.I. Bruce, D.C. Kehoe, J.G. Matisons, B.K. Nicholson, P.H. Rieger, M.L. Williams, *J. Chem. Soc., Chem. Commun*. (1982) 442.
17. A. Nafady, W.E. Geiger, *Organometallics* 27 (2008) 5624.
18. S.I**.** Al-Saeed, A.M. Alsalme, A. Nafady, *Int. J. Electrochem. Sci.* 10 (2015) in press
19. R.J. LeSuer, W.E. Geiger, *Angew. Chem., Int. Ed.* 39 (2000) 248.
20. W.E. Geiger, "*In Laboratory Techniques in Electroanalytical Chemistry",* 2nd ed.; P.T. Kissinger, W.R. Heineman, Eds.; Marcel Dekker: New York, (1996); Chapter 23.
21. C.G. Zoski, D.A. Sweigart, N.J. Stone, P.H. Rieger, E. Mocellin, T.F. Mann, D.R. Mann, D.K. Gosser, M.M. Doeff, A.M. Bond, *J. Am. Chem. Soc*. 110 (1988) 2109.
22. J.W. Hershberger, C. Amatore, J.K. Kochi, *J organomet. Chem*. 250 (1983) 345.
23. B.T. Donovan, W.E. Geiger, *J. Am. Chem. Soc*. 110 (1988) 2335.